

# New PhotoElectric effect model for GeantV/Geant4

Marilena Bandieramonte

CERN

*marilena.bandieramonte@cern.ch*

September 5, 2017

# Overview

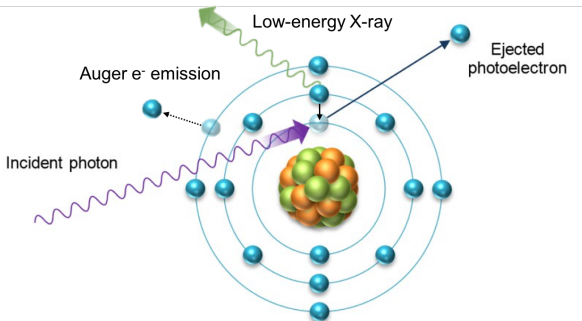
- 1 PhotoElectric effect - Introduction
  - Introduction
- 2 PhotoElectric effect in Geant4
  - Standard electromagnetic package
  - Low energy package
- 3 Developing a new Photoelectric model
  - Possible actions and open points
  - Livermore model analysis
  - New parameterisation with epics2014 data
- 4 Verification results
- 5 Conclusions
- 6 Appendix

# Introduction

In the photo-electric absorption process a **photon is absorbed** by an atom and an **electron is emitted** with an energy:

$$E_{photoelectron} = E_{\gamma} - B_{shell}(Z_i) \quad (1)$$

The atom, left in an excited state with a vacancy in the ionized shell, decays to its ground state through a cascade of radiative and non-radiative transitions with the **emission of characteristic x-rays** and **Auger and Coster-Kronig electrons**.



## PhotoElectric effect in Geant4

# Geant4 photoelectric package

The basic set of gamma models in EM physics packages [J Allison , 2016] [V. Ivanchenko, 2011] includes:

# Geant4 photoelectric package

The basic set of gamma models in EM physics packages [J Allison , 2016] [V. Ivanchenko, 2011] includes:

- Models developed for HEP applications: **standard electromagnetic package**
  - *G4PEEffectFluoModel*: V. Grichine, M. Mairie and V. Ivanchenko

# Geant4 photoelectric package

The basic set of gamma models in EM physics packages [J Allison , 2016] [V. Ivanchenko, 2011] includes:

- Models developed for HEP applications: **standard electromagnetic package**
  - *G4PEEffectFluoModel*: V. Grichine, M. Mairie and V. Ivanchenko
- Models based on the **Livermore** evaluated data Library
  - *G4LivermorePhotoElectricModel*: A Ivanchenko and V. Ivanchenko
  - *G4LivermorePolarizedPhotoElectricModel*: Sebastien Incerti, A.Forti, M.G.Pia, A. Mantero and V. Ivanchenko
- C++ implementation of the **Penelope** 2001 models
  - *G4PenelopePhotoElectricModel*: L. Pandola

If photon energy is below the lowest available energy, the cross section is computed for this lowest energy, to ensure the **gamma is absorbed by photoabsorption at any energy**.

- This is done for transport reasons in HEP
- As a result, all media is non-transparent to low-energy gamma rays

# Standard electromagnetic package: G4PEEffectFluoModel

- **The atomic cross sections.** Biggs et al. parameterization from SANDIA tables, with separate fit of coefficients, is used :

$$\sigma(Z, E_\gamma) = \frac{a(Z, E_\gamma)}{E_\gamma} + \frac{b(Z, E_\gamma)}{E_\gamma^2} + \frac{c(Z, E_\gamma)}{E_\gamma^3} + \frac{d(Z, E_\gamma)}{E_\gamma^4} \quad (2)$$

- **The sub-shell** it's chosen in a **deterministic way**, not sampled:
  - the first inner shell having a binding energy  $B_{shell} < E_\gamma$
- Shell atomic energies are taken from *G4AtomicShells* data
- **The photoelectron angle** is calculated according to the Sauter-Gavrila distribution for K shell, which is correct only to zero order in  $\alpha Z$



# Low Energy Package: G4LivermorePhotoElectricModel

- The **total photoelectric and single shell cross-sections** are tabulated from threshold to 600keV. Above 600keV EPDL97 cross sections are parameterised as following:

$$\sigma(E) = \frac{a_1}{E} + \frac{a_2}{E^2} + \frac{a_3}{E^3} + \frac{a_4}{E^4} + \frac{a_5}{E^5} \quad (3)$$

- The accuracy of such parameterisation is better than 1%.
- The **sub-shell** is sampled according to the relative cross-sections of all sub-shells.
- Two **angular generators**:
  - *G4SauterGavrilaAngularDistribution*: same as in the standard model - default option
  - *G4PhotoElectricAngularGeneratorPolarized*: double differential cross section generator derived from Gavrila's calculations, which can also handle polarized photons.

# Low Energy Package: G4PenelopePhotoElectricModel

- The **total photoelectric cross section** at a given photon energy  $E$  is calculated from the data EPDL89 [D.E.Cullen , 1989].

# Low Energy Package: G4PenelopePhotoElectricModel

- The **total photoelectric cross section** at a given photon energy  $E$  is calculated from the data EPDL89 [D.E.Cullen , 1989].
- The **sub-shell** is selected according to the relative cross sections of sub-shells, determined at the energy  $E$  by interpolation of the data. Only K-L-M shells are taken into account.

# Low Energy Package: G4PenelopePhotoElectricModel

- The **total photoelectric cross section** at a given photon energy  $E$  is calculated from the data EPDL89 [D.E.Cullen , 1989].
- The **sub-shell** is selected according to the relative cross sections of sub-shells, determined at the energy  $E$  by interpolation of the data. Only K-L-M shells are taken into account.
- The **direction of the electron** is sampled according to the Sauter distribution. Introducing the variable  $\nu = 1 - \cos\theta_e$ , the angular distribution can be expressed as:

$$p(\nu) = (2 - \nu) \left[ \frac{1}{A + \nu} + \frac{1}{2} \beta \gamma (\gamma - 1) (\gamma - 2) \right] \frac{\nu}{(A + \nu)^3} \quad (4)$$

where

$$\gamma = 1 + \frac{E_e}{m_e c^2}, \quad A = \frac{1}{\beta} - 1 \quad (5)$$

where  $E_e$  is the electron energy,  $m_e$  its rest mass and  $\beta$  its velocity in units of the speed of light  $c$ .

## New G4/GV photoelectric models development

# Possible actions and open points

# Possible actions and open points

- **Revert to original Sandia coefficients:** not an option. Sandia parameterization is not statistically superior to EPDL. Furthermore subshells cross sections are missing and the selection is currently done in a deterministic way.

# Possible actions and open points

- **Revert to original Sandia coefficients:** not an option. Sandia parameterization is not statistically superior to EPDL. Furthermore subshells cross sections are missing and the selection is currently done in a deterministic way.
- **Use EPDL/livermore in standard physics:** livermore model is more complex (but also more accurate) than the current standard. It can be improved:
  - Accuracy of cross-sections with new available data (livermore/epics2014)
  - CPU performance
  - Angular generator sampling algorithm



# Possible actions and open points

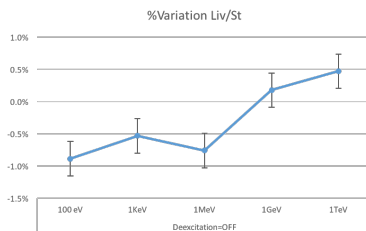
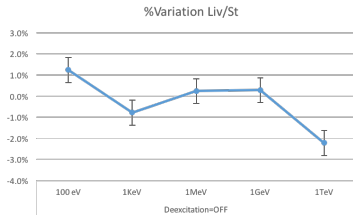
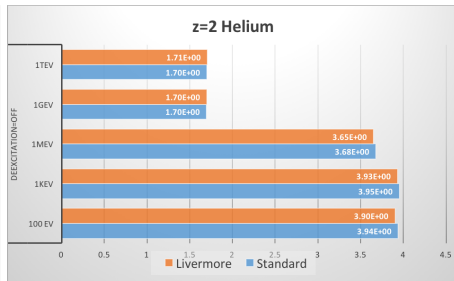
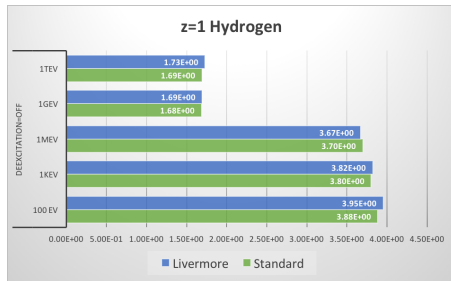
- **Revert to original Sandia coefficients:** not an option. Sandia parameterization is not statistically superior to EPDL. Furthermore subshells cross sections are missing and the selection is currently done in a deterministic way.
- **Use EPDL/livermore in standard physics:** livermore model is more complex (but also more accurate) than the current standard. It can be improved:
  - Accuracy of cross-sections with new available data (livermore/epics2014)
  - CPU performance
  - Angular generator sampling algorithm
- Other possibilities under investigation:
  - **Move to Ebel's parametrization:** K- shell cross sections based on Ebel's parameterisation produce more accurate results than EPDL in some test cases close to absorption edges for energy range [1KeV- 300 KeV]

# Possible actions and open points

- **Revert to original Sandia coefficients:** not an option. Sandia parameterization is not statistically superior to EPDL. Furthermore subshells cross sections are missing and the selection is currently done in a deterministic way.
- **Use EPDL/livermore in standard physics:** livermore model is more complex (but also more accurate) than the current standard. It can be improved:
  - Accuracy of cross-sections with new available data (livermore/epics2014)
  - CPU performance
  - Angular generator sampling algorithm
- Other possibilities under investigation:
  - **Move to Ebel's parametrization:** K- shell cross sections based on Ebel's parameterisation produce more accurate results than EPDL in some test cases close to absorption edges for energy range [1KeV- 300 KeV]
  - **Salvat and Sabatucci** new formulation (Penelope 2015 version): uses the same theory as in Scofield (1973) of the EPDL tables, but more accurate numerical algorithms.

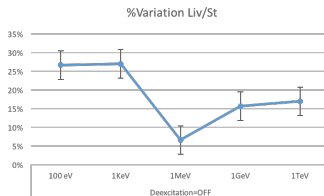
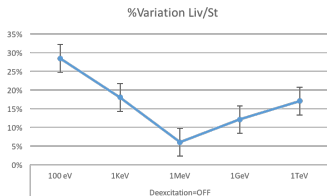
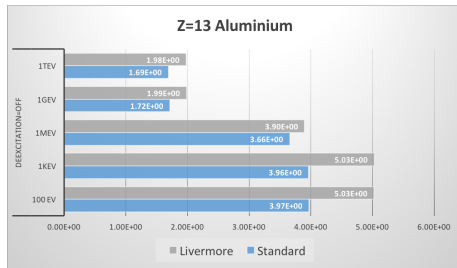
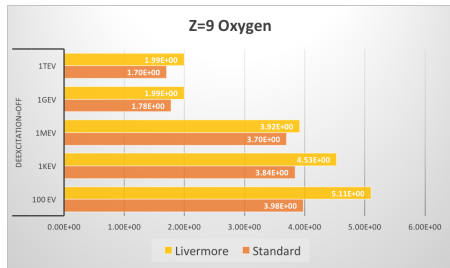
# Livermore vs Standard - execution time

Model level test,  $\#particles = 10^7$ ,  $\#repetitions = 10$



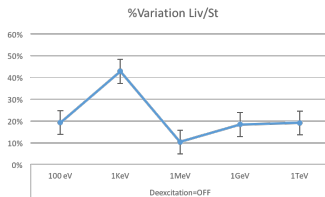
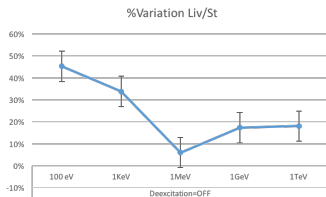
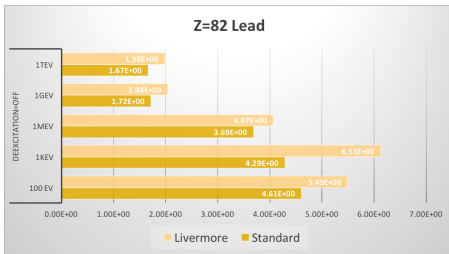
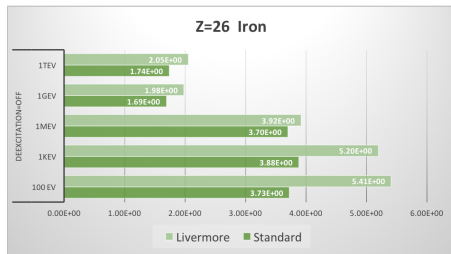
# Livermore vs Standard - execution time

Model level test,  $\#particles = 10^7$ ,  $\#repetitions = 10$



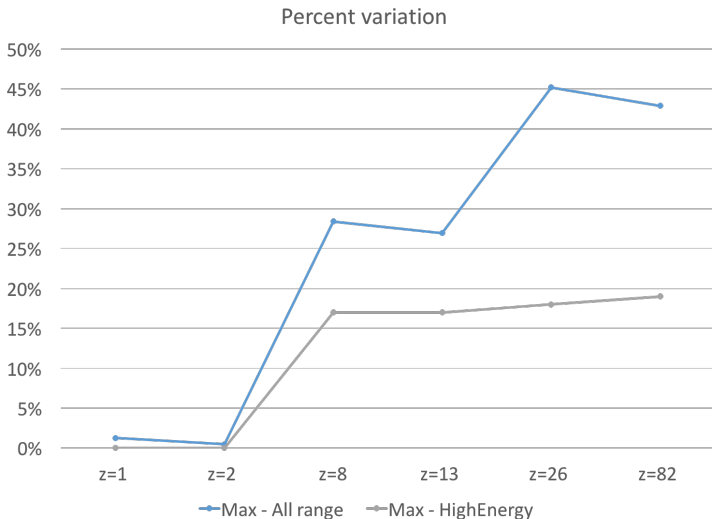
# Livermore vs Standard - execution time

Model level test,  $\#particles = 10^7$ ,  $\#repetitions = 10$

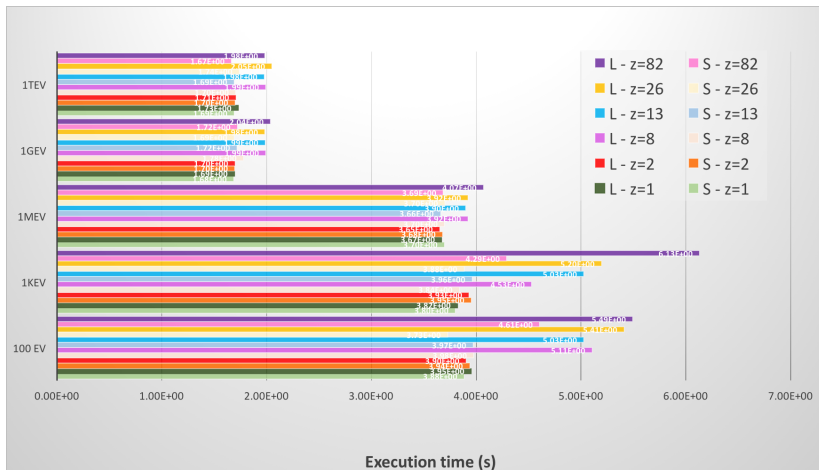


# Livermore vs Standard percent variation

Max percent variation: all energies vs  $E \geq 1\text{MeV}$

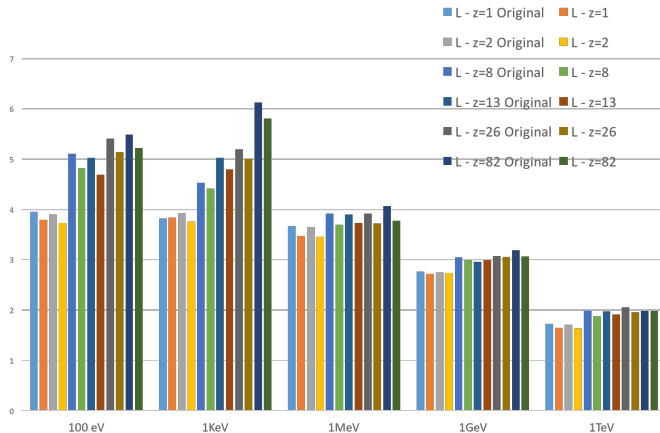


# Livermore vs Standard - Angular distribution ON



- The standard angular distribution has a threshold at  $\sim 26\text{MeV}$
- Greater differences are observable at low energies and for heavier elements

# New Penelope-like angular distribution



## Achievements:

- Increased threshold from 26MeV to 100MeV
- Speedup between 4% and 10% in most cases



# Unit test and benchmark of improved PELivermore model

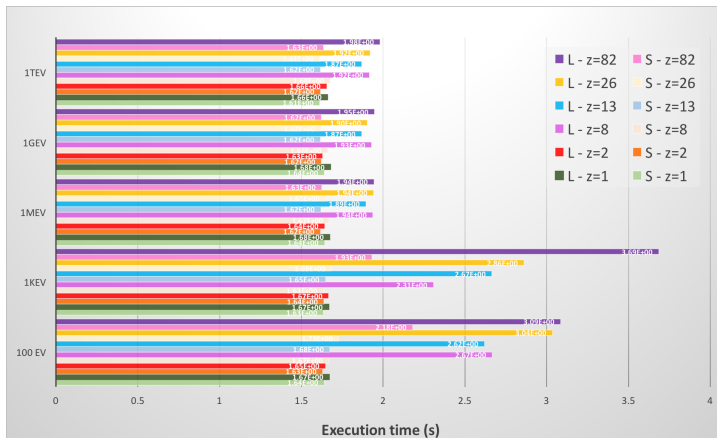
The improved Livermore model has been included in 10.3ref04 and tested:

- Results for 10.3ref04 are **stable** compared to 10.3ref03
- No visible degradation of any result
- Validation results available at  
<https://geant4-tools.web.cern.ch/geant4-tools/emtesting/>

Version 10.3ref04 with Livermore model for Rayleigh and Photo-effect used as default in Em physics list, to check **CPU performance**:

- Improved quality of photon cross sections that may slightly affect shower shape
  - 1% slowdown for Higgs sample
  - 2% slowdown for e- showers
- > Optimization on photoelectric model might recover CPU performance.

# Livermore vs Standard - Angular distribution OFF

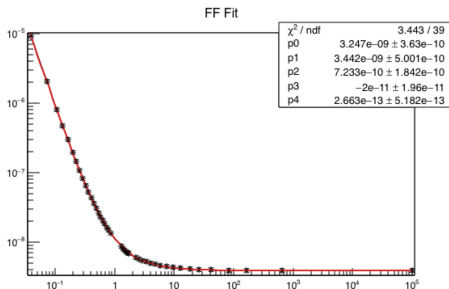


- Switching off the angular distribution we clearly see a dependency on the **energy** and on the **Z** of the material.
- This is dependent on a 600KeV threshold between tabulated and parameterised cross sections (EPDL97)

# New parameterisation - livermore/epics2014 data

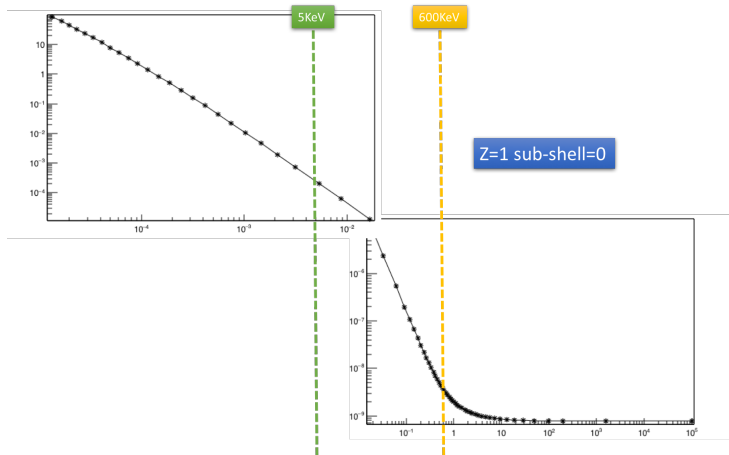
- New cross sections data recently introduced in Geant4: livermore/epics2014 (S. Incerti)
- New fit: adding one more parameter and performing two separate fits we can reduce the threshold from 600KeV to 5KeV.

$$\sigma(E) = \frac{a_1}{E} + \frac{a_2}{E^2} + \frac{a_3}{E^3} + \frac{a_4}{E^4} + \frac{a_5}{E^5} + \frac{a_6}{E^6} \quad (6)$$



- $E_\gamma \geq 5\text{KeV}$ : Two new fits in two different energy ranges
  - $E_\gamma \in [5\text{KeV} - 50\text{KeV}]$
  - $E_\gamma > 50\text{KeV}$
- $E_\gamma < 5\text{KeV}$ :
  - Keep the parameterisation (under evaluation): high-energy physics simulations
  - Tabulated cross sections: low-energy physics simulations

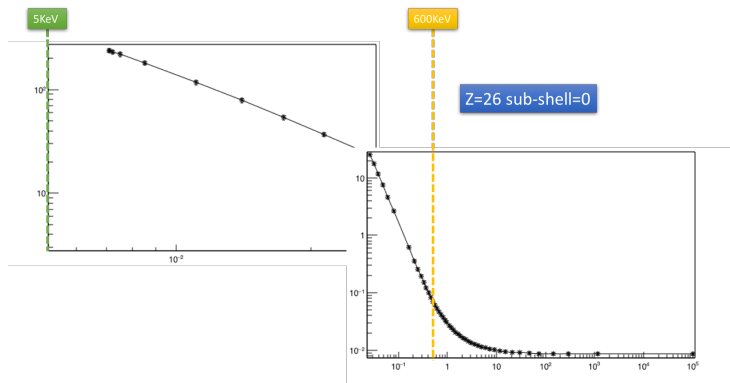
# Two separate fits - new data



## Achievements:

- Threshold moved from 600KeV to 5KeV
- Speedup measured (following slides)

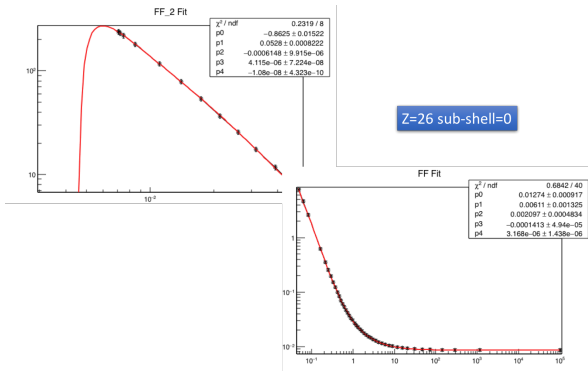
# Two separate fits - new data



- In some cases we are able to cover all the spectrum with parameterization
- Especially for inner shells

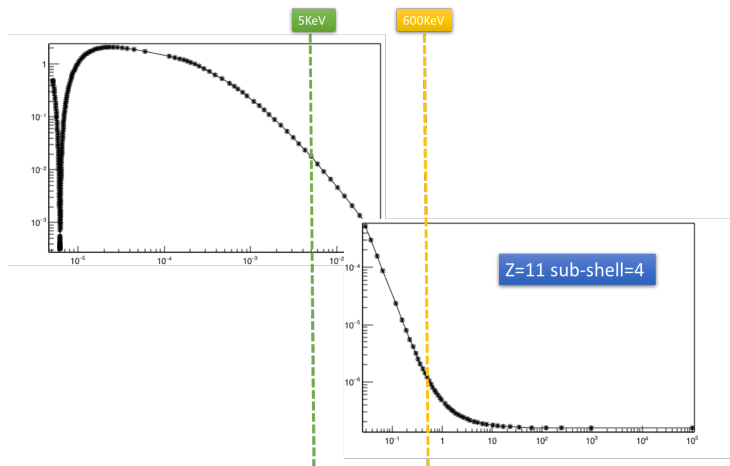
# New parameterisation: example

- Two threshold limits: lowLim and highLim dynamically set.
- The continuity is assured fixing one parameter of the low energy fit, forcing it to be equal to the first point of the high-energy fit.
- HighLim threshold is then set to the closest real point available in the cross-section file.

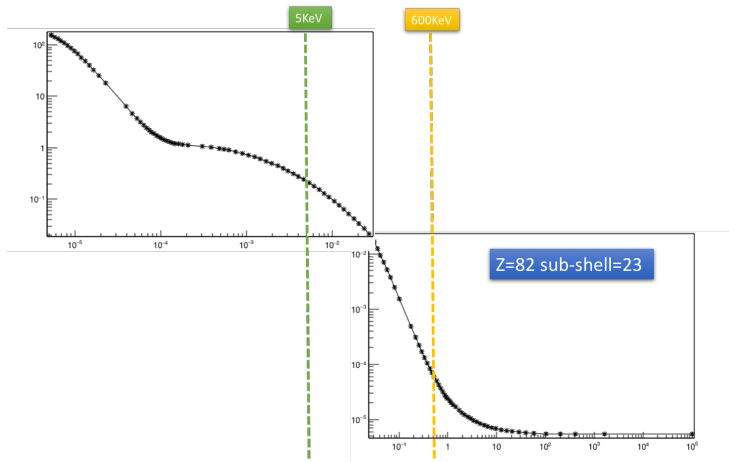


# Two separate fits - new data: special cases

- Outer shells present a non-monotonic behaviour, significantly at very low energies



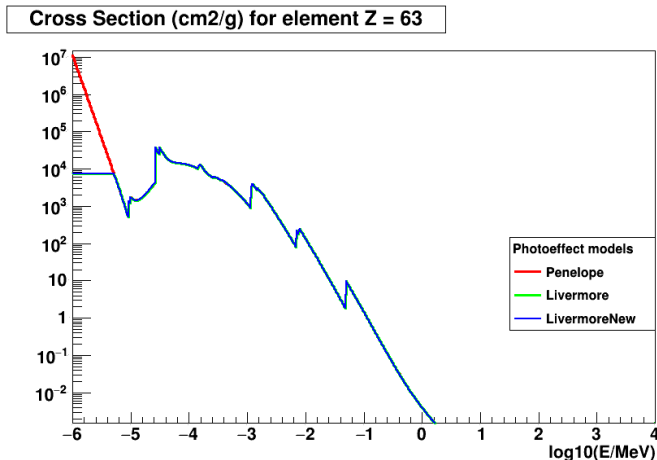
# Two separate fits - new data: special cases





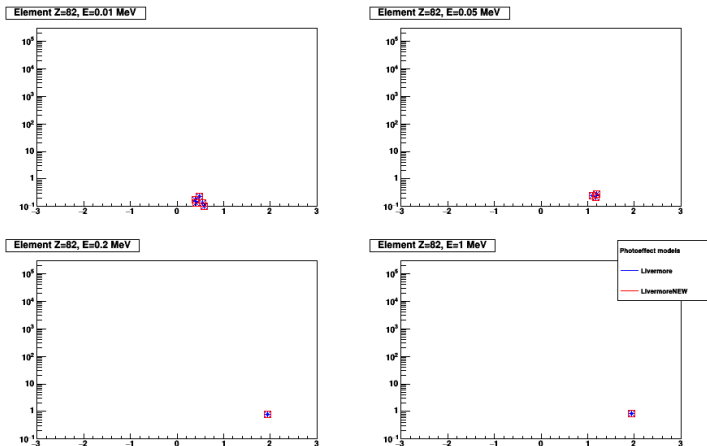
# Geant4 models Cross-sections comparison

Observed cross-sections in respect with Penelope within 5%.



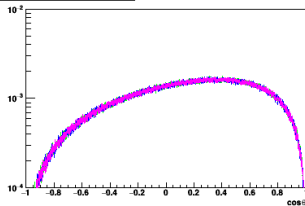
# Geant4 models photoelectron energy comparison

Electron Energy Spectra Livermore respective to beam energy (i.e.  $\log_{10}((\text{energy} - E_1)/\text{keV}))$ )

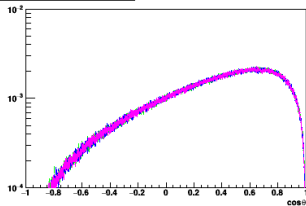


# Geant4 models photoelectron angular comparison

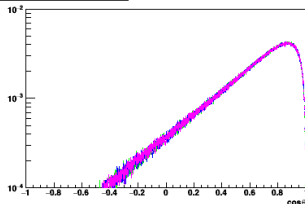
Element Z=82, E=0.01 MeV



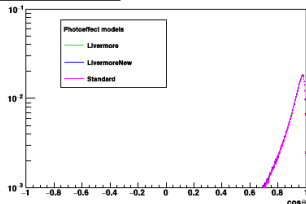
Element Z=82, E=0.05 MeV



Element Z=82, E=0.2 MeV

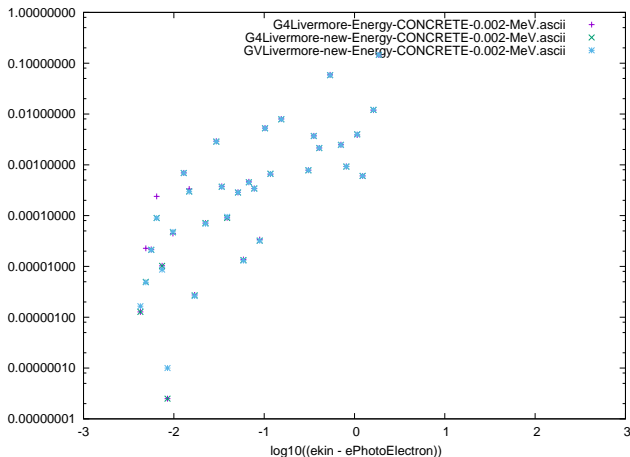


Element Z=82, E=1 MeV



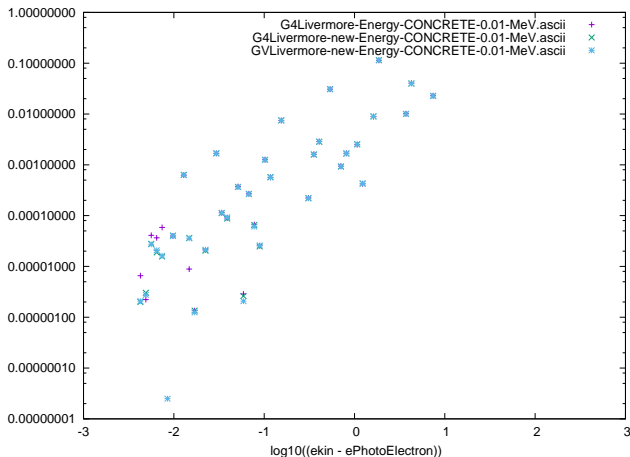
# Geant4 and GeantV models photoelectron energy comparison

Test on CONCRETE,  $E_\gamma = 0.002\text{MeV}$ ,  $\#particles = 10^7$



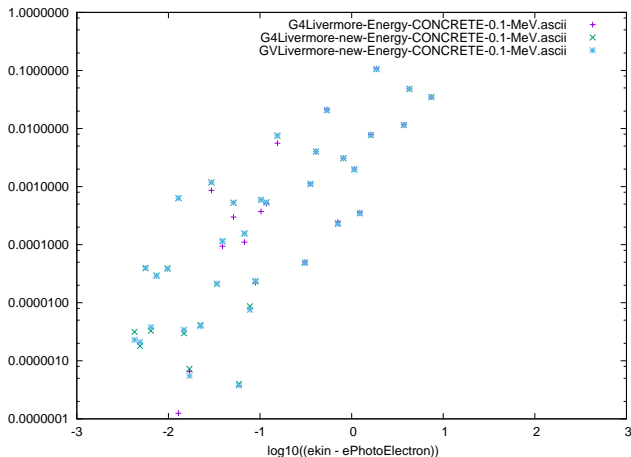
# Geant4 and GeantV models photoelectron energy comparison

Test on CONCRETE,  $E_\gamma = 0.01\text{MeV}$ ,  $\#particles = 10^7$



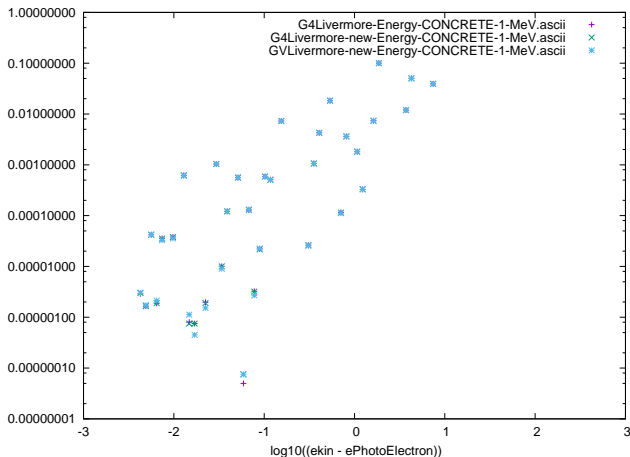
# Geant4 and GeantV models photoelectron energy comparison

Test on CONCRETE,  $E_\gamma = 0.1\text{MeV}$ ,  $\#particles = 10^7$



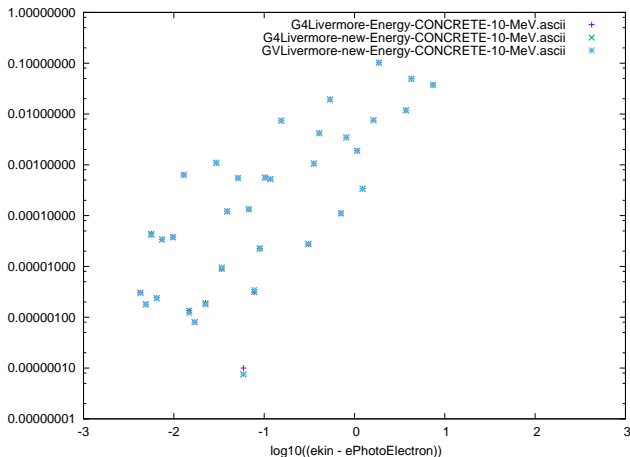
# Geant4 and GeantV models photoelectron energy comparison

Test on CONCRETE,  $E_\gamma = 1\text{MeV}$ ,  $\#particles = 10^7$



# Geant4 and GeantV models photoelectron energy comparison

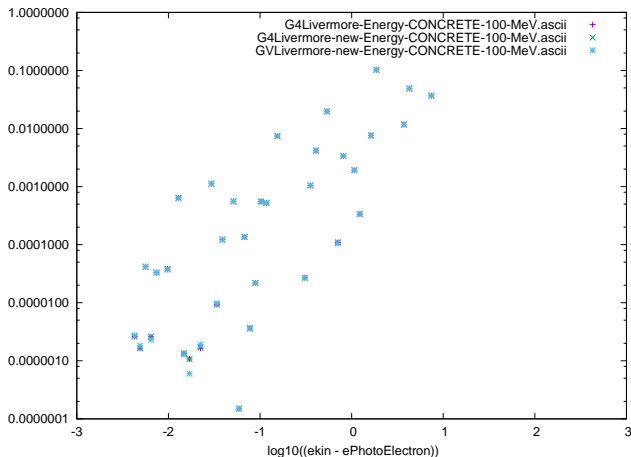
Test on CONCRETE,  $E_\gamma = 10\text{MeV}$ ,  $\#particles = 10^7$





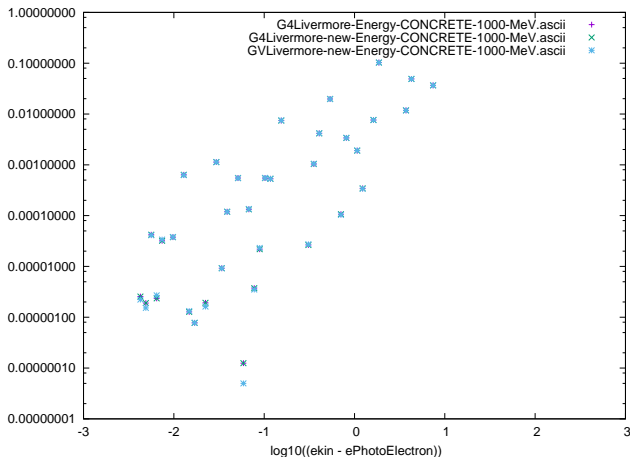
# Geant4 and GeantV models photoelectron energy comparison

Test on CONCRETE,  $E_\gamma = 100\text{MeV}$ ,  $\#particles = 10^7$



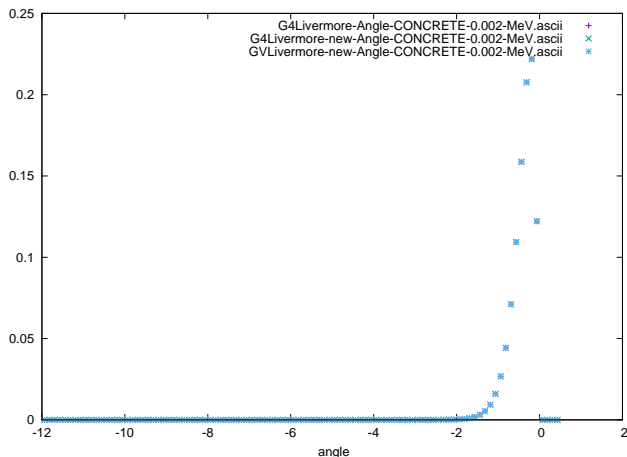
# Geant4 and GeantV models photoelectron energy comparison

Test on CONCRETE,  $E_\gamma = 1000\text{MeV}$ ,  $\#particles = 10^7$



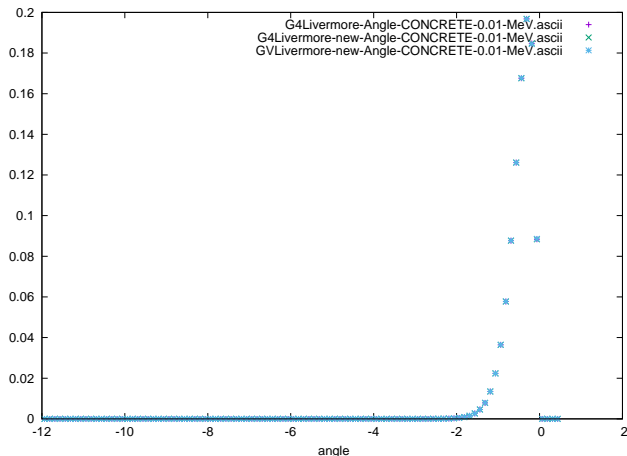
# Geant4 and GeantV models photoelectron angular distribution

Test on CONCRETE,  $E_\gamma = 0.002\text{MeV}$ ,  $\#particles = 10^7$



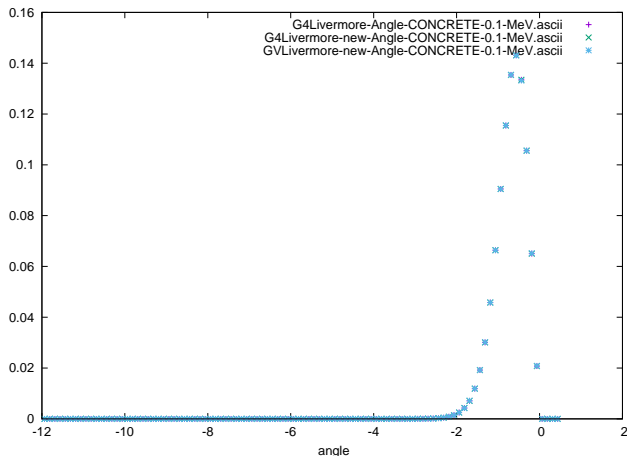
# Geant4 and GeantV models photoelectron angular distribution

Test on CONCRETE,  $E_\gamma = 0.01\text{MeV}$ ,  $\#particles = 10^7$



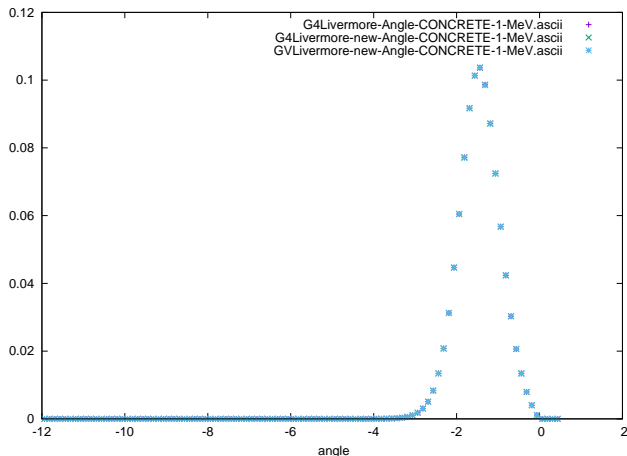
# Geant4 and GeantV models photoelectron angular distribution

Test on CONCRETE,  $E_\gamma = 0.1\text{MeV}$ ,  $\#particles = 10^7$



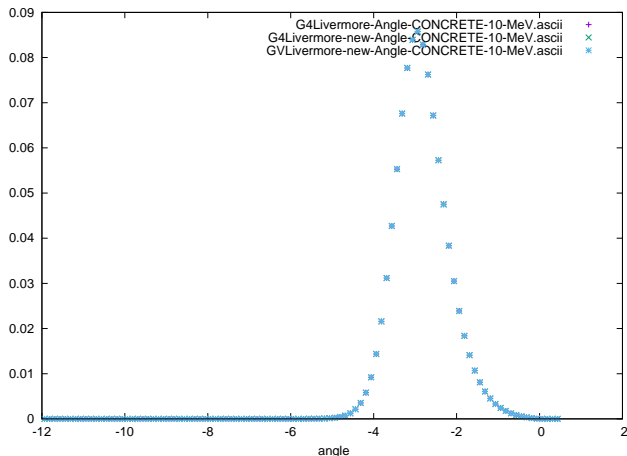
# Geant4 and GeantV models photoelectron angular distribution

Test on CONCRETE,  $E_\gamma = 1\text{MeV}$ ,  $\#particles = 10^7$



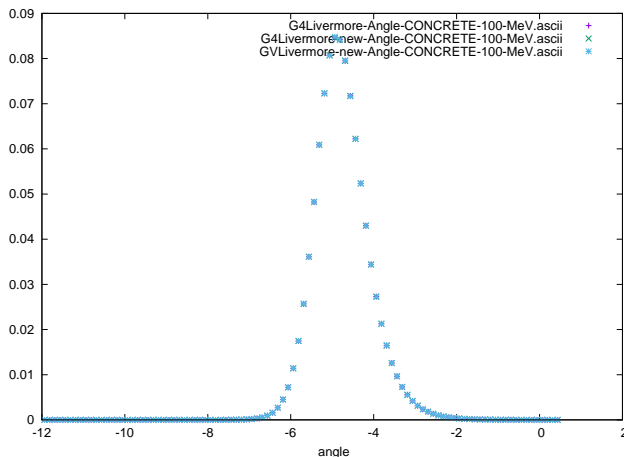
# Geant4 and GeantV models photoelectron angular distribution

Test on CONCRETE,  $E_\gamma = 10\text{MeV}$ ,  $\#particles = 10^7$



# Geant4 and GeantV models photoelectron angular distribution

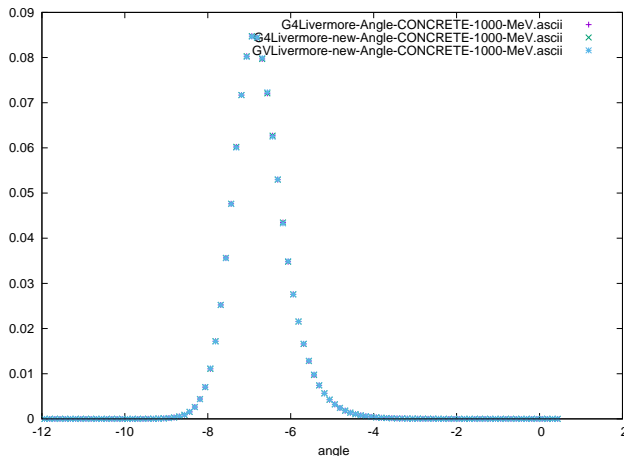
Test on CONCRETE,  $E_\gamma = 100\text{MeV}$ ,  $\#particles = 10^7$



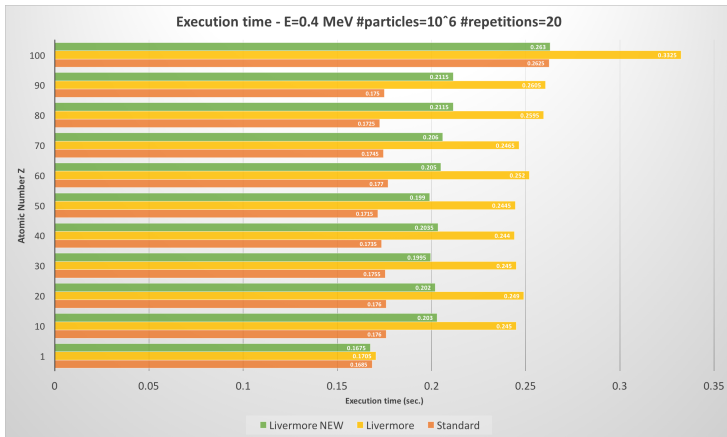


# Geant4 and GeantV models photoelectron angular distribution

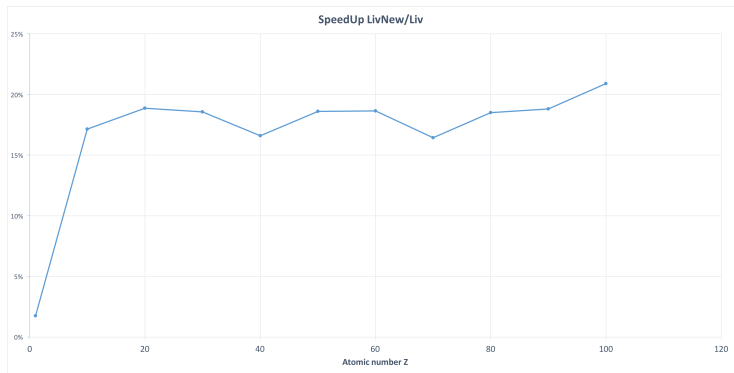
Test on CONCRETE,  $E_\gamma = 1000\text{MeV}$ ,  $\#particles = 10^7$



# New Livermore vs Standard and Livermore Execution times



# New Livermore vs Standard and Livermore Execution times



- Measured speed-up between 17% and 21%.

# Conclusions and plans

# Conclusions and plans

- Review of G4 photoelectric models has been done

# Conclusions and plans

- Review of G4 photoelectric models has been done
- Updated and improved Livermore model:
  - Photoelectron angular distribution sampling has been improved. Measurements report improvements between 4% and 10%.
    - The use of **Alias sampling** in GeantV for the rejection part will eventually produce greater gains.
  - A new fit (in two steps) on updated cross-sections data has been performed
    - More accuracy
    - More efficiency: threshold from 600KeV to 5KeV
  - The sampling of secondaries has been improved: speedup between 17% and 21%.

# Conclusions and plans

- Review of G4 photoelectric models has been done
- Updated and improved Livermore model:
  - Photoelectron angular distribution sampling has been improved. Measurements report improvements between 4% and 10%.
    - The use of **Alias sampling** in GeantV for the rejection part will eventually produce greater gains.
  - A new fit (in two steps) on updated cross-sections data has been performed
    - More accuracy
    - More efficiency: threshold from 600KeV to 5KeV
  - The sampling of secondaries has been improved: speedup between 17% and 21%.
- This model can be an alternative to the standard model (Geant4):
  - More accurate parameterization (new data)
  - That take into account shells sampling
  - Fast 'enough'

Thanks for your attention.



# Appendix

# Experimental data: Total cross sections

TABLE II  
SUMMARY OF THE EXPERIMENTAL TOTAL CROSS SECTION DATA USED IN THE VALIDATION ANALYSIS

Atomic Number	Element	Energy range (keV)	Sample size	References
1	H	0.0136 - 0.020	27	[102]–[104]
2	He	0.025 - 0.277	320	[105]–[112]
3	Li	0.046 - 0.400	93	[113]–[116]
7	N	0.015 - 0.4	73	[117], [118]
8	O	0.013 - 0.28	215	[103], [119]–[121]
10	Ne	0.022 - 2.952	448	[108], [110]–[112], [117], [122]
11	Na	0.046 - 0.246	17	[123]
13	Al	145.4	1	[124]
17	Cl	0.016 - 0.078	25	[125]
18	Ar	0.016 - 6	487	[105], [110]–[112], [117], [126]–[130]
19	K	0.004 - 0.005	12	[131]
22	Ti	59.54	1	[132]
23	V	59.54	1	[132]
24	Cr	59.54	1	[132]
25	Mn	59.54	1	[132]
26	Fe	0.008 - 59.54	25	[132]–[134]
27	Co	59.54	1	[132]
28	Ni	1.487 - 59.54	17	[132], [133]
29	Cu	59.54 - 661.6	9	[124], [132], [135]–[138]
30	Zn	59.54	1	[132]
33	As	59.54	1	[132]
34	Se	59.54	1	[132]
36	Kr	0.015 - 1.626	357	[105], [110], [112], [139], [140]
37	Rb	0.004 - 0.010	4	[141]
38	Sr	59.54	1	[132]
39	Y	279.2 - 661.6	2	[142]
40	Zr	59.54 - 661.6	7	[124], [135]–[137], [143]
41	Nb	59.54	2	[143]
42	Mo	59.54 - 661.6	7	[132], [138], [143]
43	Tc	59.54	1	[143]

# Experimental data: Total cross sections

46	Pd	59.54	1	[143]
47	Ag	1.487 - 661.6	13	[124], [?], [135]–[137], [143]–[146]
48	Cd	59.54	2	[132], [143]
49	In	59.54	2	[143]
50	Sn	1 - 661.6	31	[124], [133], [135]–[137], [143], [144], [146]
51	Sb	59.54	1	[143]
52	Te	59.54	2	[143]
54	Xe	0.013 - 6	657	[110], [122], [128], [130], [147]
55	Cs	0.004 - 59.54	14	[132], [141], [148]
57	La	59.54	1	[149]
58	Ce	59.54 - 661.6	6	[142], [149]–[152]
59	Pr	59.54 - 661.6	3	[150]–[152]
60	Nd	59.54 - 661.6	2	[150], [152]
61	Pm	59.54	1	[152]
62	Sm	59.54 - 145.4	4	[149], [151], [152]
63	Eu	59.54	2	[149], [152]
64	Gd	59.54 - 661.6	5	[150]–[153]
65	Tb	59.54	3	[149], [152], [153]
66	Dy	59.54 - 661.6	8	[142], [149]–[153]
67	Ho	59.54	1	[152]
68	Er	59.54	3	[149], [152], [153]
70	Yb	279.2 - 661.6	2	[142]
72	Hf	65.839-68.547	25	[154]
73	Ta	1.487 - 661.6	31	[124], [133], [135]–[138], [144]
78	Pt	1 - 40	25	[133]
79	Au	0.93 - 661.6	33	[133], [135]–[137], [145]
80	Hg	1173	1	[155]
82	Pb	1.487 - 1173	36	[124], [133], [135]–[137], [144]–[146], [155], [156]
92	U	1.487 - 3	4	[133]

---

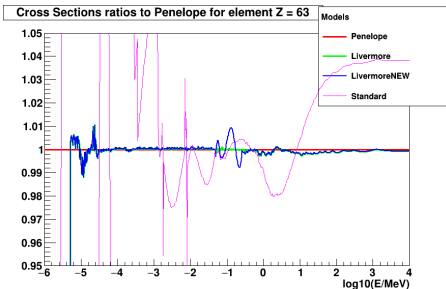
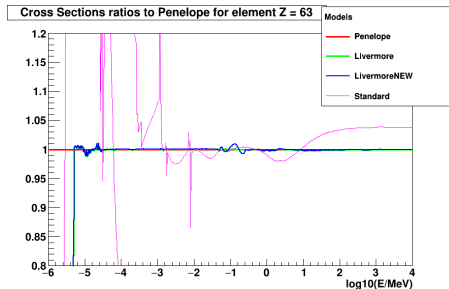
# References

-  **D.E.Cullen et al**  
Tables and graphs of photon-interaction cross sections from 10 eV to 100 GeV derived from the LLNL evaluated photon data library (EPDL)  
*Report UCRL-50400 (Lawrence Livermore National Laboratory)*
-  **J Allison et al., by the Geant4 Collaboration**  
Recent Developments in Geant4  
*Nucl. Instrum. Meth. A 835 186-225, 2016*
-  **V. Ivanchenko et al.**  
Recent Improvements in Geant4 Electromagnetic Physics Models and Interfaces  
*Progress in NUCLEAR SCIENCE and TECHNOLOGY, 2011 Vol. 2, pp.898-903,*
-  **J H Hubbell**  
Review and history of photon cross section calculations  
*Phys. Med. Biol. 51 (2006) R245-R262 .*
-  **Francesc Salvat and Jose M Fernandez-Varea**  
Overview of physical interaction models for photon and electron transport used in Monte Carlo codes  
*Metrologia 46 (2009) S112-S138 2010.*
-  **Vladimir Ivanchenko et al. (2010)**  
Recent Improvements in Geant4 Electromagnetic Physics Models and Interfaces  
*Joint International Conference on Supercomputing in Nuclear Applications and Monte Carlo 2010 618(1-3), 315 - 322.*
-  **G.A.P. Cirrone and G. Cuttone and F. Di Rosa and L. Pandola and F. Romano and Q. Zhang (2010)**  
Validation of the Geant4 electromagnetic photon cross-sections for elements and compounds  
*Nuclear Instruments and Methods in Physics Research Section A: Accelerators, Spectrometers, Detectors and Associated Equipment 618(1-3), 315 - 322.*
-  **M. C. Han and H. S. Kim and M. G. Pia and T. Basaglia and M. Batic and G. Hoff and C. H. Kim and P. Saracco (2016)**  
Validation of Cross Sections for Monte Carlo Simulation of the Photoelectric Effect  
*IEEE Transactions on Nuclear Science 63(2), 1117-1146.*

# The End

# Backup slides

# Geant4 models x-section ratio comparison



# Standard electromagnetic package - Geant4-10.2 - Final state sampling

Differential Photoelectric cross section correct to first order  $\alpha Z$

$$\frac{d\sigma}{d\cos\theta} \simeq \frac{\sin^2\theta}{(1-\beta\cos\theta)^4} \left\{ 1 + \frac{1}{2}\gamma(\gamma-1)(\gamma-2)(1-\beta\cos\theta) \right\} \quad (7)$$

where  $\beta$  and  $\gamma$  are the photoelectron Lorentz factors.  $\cos\theta$  is sampled from the probability density function :

$$f(\cos\theta) = \frac{1-\beta^2}{2\beta} \frac{1}{(1-\beta\cos\theta)^2} \quad (8)$$

so

$$\cos\theta = \frac{(1-2r) + \beta}{(1-2r)\beta + 1} \quad (9)$$

The rejection function is :

$$g(\cos\theta) = \frac{1-\cos^2\theta}{(1-\beta\cos\theta)^2} [1 + b(1-\beta\cos\theta)] \quad (10)$$

with  $b = \gamma(\gamma-1)(\gamma+1)/2$

It can be shown that  $g(\cos\theta)$  is positive for each  $\cos\theta \in [-1, +1]$ , and can be majored by :

$$g^{sup} = \begin{cases} \gamma^2[1 + b(1-\beta)] & \text{if } \gamma \in [1, 2] \\ \gamma^2[1 + b(1+\beta)] & \text{if } \gamma > 2 \end{cases} \quad (11)$$

The efficiency of this method is  $\sim 50\%$  if  $\gamma < 2$ ,  $\sim 25\%$  if  $\gamma \in [2, 3]$ .



# Standard electromagnetic package - Geant 10.2 - Macroscopic and atomic cross-sections

- Once the photoelectric process is selected, the model must choose **which atom** is involved. In compound materials the  $i^{th}$  element is chosen randomly according to the probability:

$$Prob(Z_i, E_\gamma) = \frac{n_i \sigma_i(Z_i, E_\gamma)}{\sum_i [n_i \sigma_i(E_\gamma)]} \quad (12)$$

where  $n_i$  is the number of atom per volume of the  $i^{th}$  element composing the material.

- For each process the **total cross section** at a given energy  $E$  is obtained with a log-log interpolation of cross section data  $\sigma_1$  and  $\sigma_2$  available **in the data libraries** from the closest energies.

# Macroscopic cross section and mean free path

- For compound materials (and also for mixtures) the molecular cross section  $\sigma_{ph}(E)$  is evaluated by means of the **additivity approximation**.

# Macroscopic cross section and mean free path

- For compound materials (and also for mixtures) the molecular cross section  $\sigma_{ph}(E)$  is evaluated by means of the **additivity approximation**.
- It consists in the **sum of the atomic cross sections** of all the elements in the molecule:

$$\sigma(E_\gamma) = \sum_i n_i \sigma(Z_i, E_\gamma) \quad (13)$$

where  $n_i$  is the number of atoms per volume of the  $i^{th}$  element of the material.

# Macroscopic cross section and mean free path

- For compound materials (and also for mixtures) the molecular cross section  $\sigma_{ph}(E)$  is evaluated by means of the **additivity approximation**.
- It consists in the **sum of the atomic cross sections** of all the elements in the molecule:

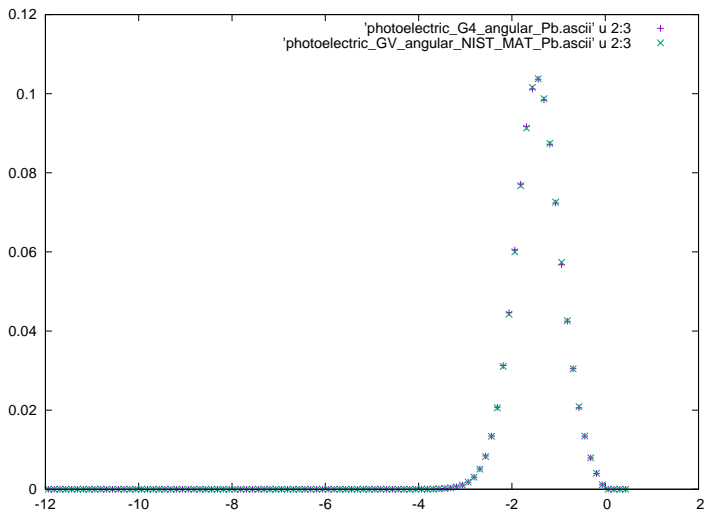
$$\sigma(E_\gamma) = \sum_i n_i \sigma(Z_i, E_\gamma) \quad (13)$$

where  $n_i$  is the number of atoms per volume of the  $i^{th}$  element of the material.

- The **mean free path**,  $\lambda$ , for a photon to interact via the photoelectric effect is given by:

$$\lambda(E_\gamma) = \left( \sum_i n_i \sigma(Z_i, E_\gamma) \right)^{-1} \quad (14)$$

# PhotoElectric SG angular distribution



# Total Photoeffect cross section correct to first order $\alpha Z$

$$\sigma_{\kappa} = \frac{3}{2} \phi_0 \alpha^4 Z^5 \frac{\beta^3 (1 - \beta^2)}{\left[1 - (1 - \beta^2)^{\frac{1}{2}}\right]^5} \left[ \mathfrak{M} \left(1 - \frac{\pi \alpha Z}{\beta}\right) + \pi \alpha Z \mathfrak{N} \right] \quad (15)$$

where

$$\mathfrak{M} = \frac{4}{3} + \frac{1 - 3(1 - \beta^2)^{\frac{1}{2}} + 2(1 - \beta^2)}{\beta^2 (1 - \beta^2)^{\frac{1}{2}}} \left[ 1 + \frac{1 - \beta^2}{2\beta} \ln \frac{1 - \beta}{1 + \beta} \right] \quad (16)$$

and

$$\begin{aligned} \mathfrak{N} = & \frac{1}{\beta^3} \left\{ -\frac{4}{15} \frac{1}{(1 - \beta^2)^{\frac{1}{2}}} \right\} + \frac{34}{15} - \frac{63}{15} (1 - \beta^2)^{\frac{1}{2}} + \frac{25}{15} (1 - \beta^2) + \\ & \frac{8}{15} (1 - \beta^2)^{\frac{3}{2}} + (1 - \beta^2)^{\frac{1}{2}} \left[ 1 - 3(1 - \beta^2)^{\frac{1}{2}} + 2(1 - \beta^2) \right] \frac{1}{2\beta} \ln \frac{1 - \beta}{1 + \beta} \end{aligned} \quad (17)$$

## Standard electromagnetic package - Geant 10.2 - Total cross-section

For each process the **total cross section** at a given energy  $E$  is obtained with a log-log interpolation.

$$\log(\sigma(E)) = \log(\sigma_1) \frac{\log(E_2) - \log(E)}{\log(E_2) - \log(E_1)} + \log(\sigma_2) \frac{\log(E) - \log(E_1)}{\log(E_2) - \log(E_1)} \quad (18)$$

where  $E_1$  and  $E_2$  are the closest lower and higher energy for which cross section data  $\sigma_1$  and  $\sigma_2$  are available **in the data libraries** respectively.

- According to G4PEFluoModel for energies  $E_\gamma > 25.55\text{MeV}$  it is assumed that the emitted photoelectron has the same direction as the incident gamma. This means that for  $E_\gamma > 25.55\text{MeV}$   $\cos\theta = 1$  always.
- N.B.: Need to test/check and correct the number of bin and the number of tested energies. (with nBins=200 there aren't improvements with respect to nBins=151 which is working better than nBin=99)
- Da  $0.5\text{MeV}$  in su abbiamo problemi nel riprodurre la distribuzione angolare. Update: Improved, but still need to test.



# Photoelectric effect in Geant4 - low energy package

Two implementations of the p.e. effect. The Livermore and Penelope cross-sections are tabulated according to EPDL97 and EPDL89

[D.E.Cullen , 1989], respectively.

- **G4Livermore** model provides two options of computing the angular distribution of the emitted photoelectron

# Photoelectric effect in Geant4 - low energy package

Two implementations of the p.e. effect. The Livermore and Penelope cross-sections are tabulated according to EPDL97 and EPDL89 [D.E.Cullen , 1989], respectively.

- **G4Livermore** model provides two options of computing the angular distribution of the emitted photoelectron
  - Based on **Gavrila's** distribution of the polar angle for the **K shell** and the **L1 sub-shell** - default as the standard model
  - Based on a **double differential cross section** derived from Gavrila's calculations, which can also handle polarized photons.

# Photoelectric effect in Geant4 - low energy package

Two implementations of the p.e. effect. The Livermore and Penelope cross-sections are tabulated according to EPDL97 and EPDL89 [D.E.Cullen , 1989], respectively.

- **G4Livermore** model provides two options of computing the angular distribution of the emitted photoelectron
  - Based on **Gavrila's** distribution of the polar angle for the **K shell** and the **L1 sub-shell** - default as the standard model
  - Based on a **double differential cross section** derived from Gavrila's calculations, which can also handle polarized photons.
- **G4Penelope** model is reengineered from the 2001 Penelope code.